Complementary Photocatalytic Toolbox: Control of Intramolecular *endo*- versus *exo*-trig Cyclizations of α-Phenyl Olefins to Oxaheterocyclic Products

Fabian Weick
Desirée Steuernagel
Arina Belov
Hans-Achim Wagenknecht*

Institute of Organic Chemistry, Karlsruhe Institute of Technology (KIT), Fritz-Haber-Weg 6, 76131 Karlsruhe, Germany
Wagenknecht@kit.edu

Dedicated to Shunichi Fukuzumi on his 70th birthday.

Published as part of the Cluster
Organic Photoredox Catalysis in Synthesis – Honoring Prof. Shunichi Fukuzumi's 70th Birthday

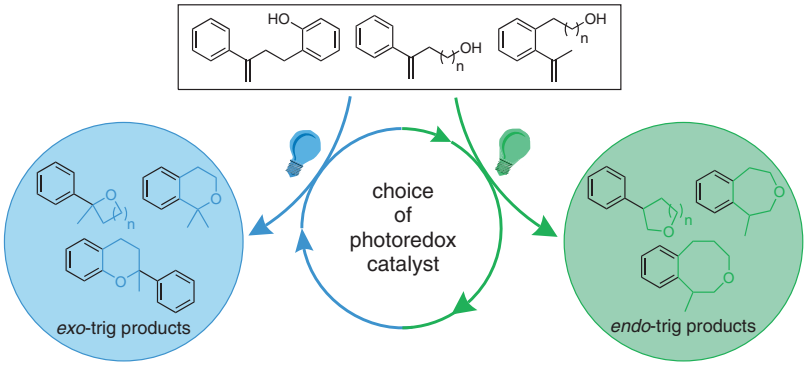

Received: 31.08.2021
Accepted after revision: 20.10.2021
Published online: 24.01.2022
DOI: 10.1055/s-0040-1719871; Art ID: st-2021-v0312-c

Crowd-Reviewed

Abstract The regioselectivity of the intramolecular cyclization of bifunctional α-phenyl alkenes can be controlled simply by the choice of the organic chromophore as the photocatalyst. The central photoredox catalytic reaction in both cases is a nucleophilic addition of the hydroxy function to the olefin function of the substrates. *N*,*N*-(4-Diisobutylaminophenyl)phenothiazine catalyzes *exo*-trig cyclizations, whereas 1,7-dicyanoperylene-3,4,9,10-tetracarboxylic acid bisimides catalyze *endo*-trig additions to products with anti-Markovnikov regioselectivity. We preliminarily report the photoredox catalytic conversions of 11 representative substrates into 20 oxaheterocycles in order to demonstrate the similarity, but also the complementarity, of these two variants in this photoredox catalytic toolbox.

Key words photochemistry, photocatalysis, perylene bisimide, phenothiazine, nucleophilic addition, cyclization

Chemical photocatalysis uses light as an energy source for organic chemical reactions. In particular, photoredox catalysis is an important concept that applies UV or visible light to generate radical anions or cations as reactive intermediates.[1] Photoredox catalysis either provides important alternatives to conventional thermal reactions or expands the repertoire of organic reactions.[2] The current workhorses for photoredox catalysis are ruthenium and iridium complexes, due to their versatile photoredox properties and photochemical robustness.[1,2] The advantage of these transition-metal photoredox catalysts is that they can be either oxidatively or reductively quenched, depending on the substrates. In contrast, organic photocatalysts cannot be similar applied to different types of organic reactions; 'the organic photocatalyst' does not exist for a wide range of different reductive or oxidative reactions.[3] Currently eosin Y,[4] flavin,[5] rhodamine 6G,[6] mesityl-[7] and aminoacridiniums,[8] naphthochromenones,[9] 4,6-dicyanobenzenes,[10] pyrimidopteridines,[11] and thioxanthones[12] have been used as organic photocatalysts and can be considered, taken together, as a photocatalytic toolbox.

Oxaheterocycles play an important role in medicinal chemistry; in particular, tetrahydropyrans and tetrahydrofurans are the most often used ring substructures.[13] Tetrahydropyrans and chromanes are also important structural motifs in natural products.[14] Due to their biological activity and effectiveness against a number of diseases, these substances are at the focus of organic syntheses.[15,16] Recently, several groups have synthesized these compounds through cobalt-[17], indium-,[18] and palladium-catalyzed[19] reactions. Intramolecular cyclizations by photocatalysis complement this synthetic toolbox and provide experimentally very similar but more-sustainable alternatives based on metal-free photoredox catalysis. We have established 1-(*N*,*N*-dimethylamino)pyrene (**APy**),[20,21] *N*-arylphenothiazines, and 1,7-dicyanoperylene-3,4,9,10-tetracarboxylic acid bisimides as organic catalysts in the photocatalytic toolbox for the alkoxylation of α-phenyl and other alkenes.[22] In particular, *N*,*N*-(4-diisobutylaminophenyl)phenothiazine (**1**) is one of the most strongly reducing photoredox catalysts reported in the literature, and yields products with Markovnikov orientation. On the other hand, 1,7-dicyanoperylene-3,4,9,10-tetracarboxylic acid bisimides photocatalyze additions to products with an anti-Markovnikov orientation.[20] The latter reactions require thiophenol as an additive and hydrogen-

atom donor. Herein, we provide a preliminary report on the cyclization of bifunctional α-phenyl alkenes by intramolecular nucleophilic addition (Figure 1).

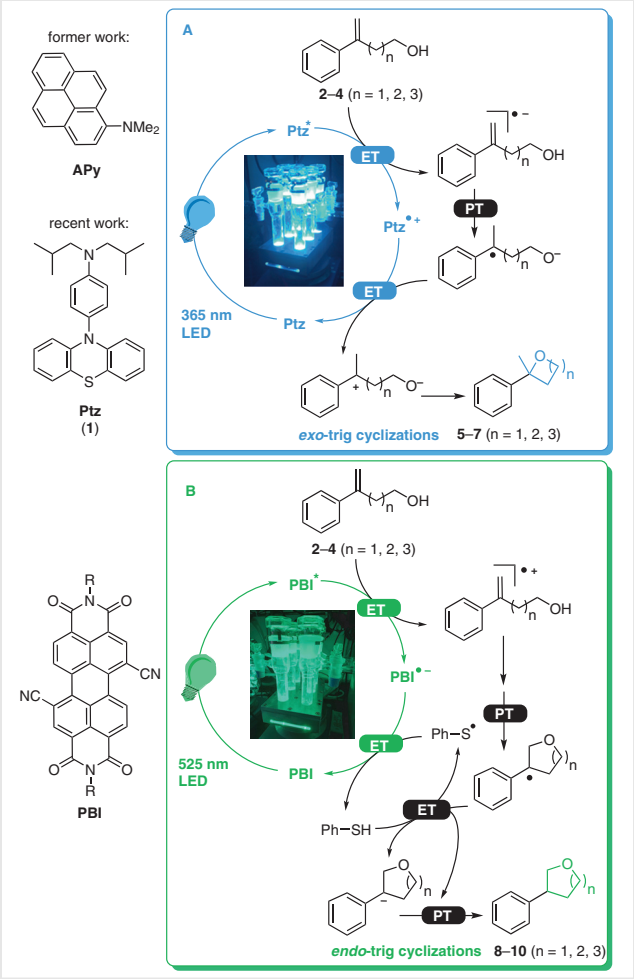

Figure 1 Two complementary, but experimentally very similar routes for photoredox-catalyzed cyclizations of α-phenylstyrenes **2–4** (*n* = 1–3) by intramolecular nucleophilic addition. The photoredox catalytic reduction of substrates **2–4** by the electron-rich *N*-arylphenothiazine **Ptz**, like **1**, with irradiation at 365 nm yields the *exo*-trig cyclized products **5–7** (top), whereas the oxidation of substrates **2–4** by an electron-deficient perylenebisimide **PBI**, irradiated at 525 nm, gives the *endo*-trig cyclized products **8–10** (bottom). ET = electron transfer; PT = proton transfer.

Perylene bisimides are soluble in CH_2Cl_2 but generally have poor solubility or are even insoluble in MeCN, the preferred polar solvent for photocatalyzed reactions. To use 1,7-dicyanoperylene-3,4,9,10-tetracarboxylic acid bisimides as photocatalysts, we had to improve their solubility. We prepared the perylene bisimides **14a–j**, differing in the substituents on the imide nitrogen (Figure 2, top). Their syntheses began from 1,7-dibromoperylene-3,4,9,10-tetracarboxylic acid dianhydride (**11**),[23] which was modified with the various substituted imide functions.[24,25] The two cyano substituents were introduced into **13a–j** by treatment with zinc(II) cyanide and a Pd catalyst.[26–28] The solubilities of the pure perylene bisimides **14a–j** were determined by preparing their saturated solutions in pure MeCN. The absorbance was measured directly after filtration of the solution or after further dilution if the optical density in a cuvette with a 1 cm path length exceeded 1.[29] The perylene bisimides with the lowest solubilities of <10 μmol/L are **14a** and **14f** (Figure 2, bottom). Obviously, the solubility was only enhanced for imides with secondary substituents, such as **14b**, **14c**, **14g**, and **14h** (~20 μmol/L), and was further enhanced for **14d**, **14e**, and **14i** (~30 μmol/l). The perylene bisimide **14j** had the best solubility (1.43 mmol/L) and was used in the subsequent photocatalytic experiments.

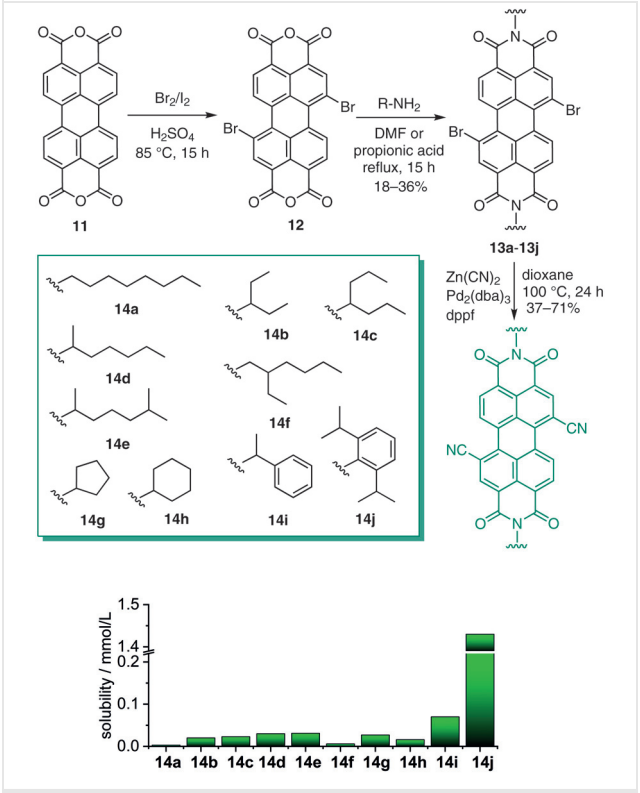

Figure 2 Synthesis (top) and solubilities in MeCN (bottom) of perylene bisimides **14a–j**. dppf = 1,1′-bis(diphenylphosphinyl)ferrocene.

The *N*-arylphenothiazine **1** is a strongly reducing photocatalyst with an excited-state oxidation potential of approximately $E_{ox}(\mathbf{1}^{\bullet+}/\mathbf{1}^{*}) = -2.9$ V (vs. SCE).[22] Accordingly, the intramolecular cyclization by **1** as photocatalyst starts with photoinduced reduction of the substrate, representatively shown for **2–4** (Figure 1). The reduction potentials of these substrates lie in the range between that of α-phenylstyrene, $E_{red}(S/S^{\bullet-}) = -2.3$ V, and that of styrene, $E_{red}(S/S^{\bullet-}) = -2.6$ V.[30] The driving force ΔG for this initial electron-transfer process can be estimated from the Rehm–Weller equation $\Delta G = E_{ox} - E_{red} - E_{00}$ (omitting the Coulombic interaction energy

E_c), and clearly lies in the negative range between –0.3 and –0.6 eV. The substrate radical anion formed after the photoinduced electron transfer undergoes instantaneous proton transfer and back electron transfer to the zwitterion, which then reacts intramolecularly to give a final cyclization product, such as **5**–**7** (Figure 3). The mesomeric stabilization of the latter cation explains the Markovnikov regioselectivity, which corresponds to an *exo*-trig cyclization. The conversion was completed after 65 hours of irradiation, as representatively shown with substrate **3** [see Supporting Information (SI), Figure S1].[31] The four-membered ring of product **5** is not formed from substrate **2**.[32] The photocatalysis gives good yields of 51–75% for the five- and six-membered rings in products **6** and **7** from substrates **3**[32] and **4**,[32] and for the benzo-fused six-membered rings in products **20** and **40** from substrates **19**[18] and **39**,[16] all according to Baldwin's rules.[33] Substrate **22**[34] is converted into the benzo-fused seven-membered ring **23**. To further broaden the scope, we used substrates **25**–**28**[32,35] and **36**[32] with variously modified phenyl groups. These were all converted into the expected *exo*-trig products in good yields. The occurrence of the byproducts **15**–**17** supports a photocatalytic mechanism, because these compounds are formed by simple deprotonation (elimination) from the cationic intermediates after back electron transfer.

The perylene bisimide **14j** is a strongly oxidizing photocatalyst with an excited-state reduction potential of E_{red}(**14j***/**14j**$^{\bullet-}$) = 2.1 V.[36] With the oxidation potential of α-phenylstyrene as a reference substrate, $E_{ox}(S^{\bullet+}/S)$ = 1.7 V,[37] the driving force is estimated to be ΔG = –0.4 V. After this initial photoinduced electron transfer, an intramolecular nucleophilic attack occurs in the radical cations of the substrate, representatively shown for substrate **3** (Figure 1). Thereby, the anti-Markovnikov regioselectivity is controlled, which is equivalent to an *endo*-cyclization. Back electron transfer and proton transfer give the six-and seven-membered rings in products **9** and **10** in good yields (88% and 43%, respectively) from substrates **3**[32] and **4**.[32] The yield of the five-membered ring in product **8** from substrate **2**[32] is low (16%) and the reaction needs further optimization. Here also, the occurrence of the byproduct **18** supports a photocatalytic mechanism, because it is formed by cyclization after a 1,3-H shift in the intermediate to the higher substituted cation. Substrates **19**[18] and **22**[34], bearing an alkylhydroxy group in the position *ortho* to the vinyl substituent, are converted into the benzo-fused seven-membered ring **21** in 63% yield and into the benzo-fused eight-membered ring in **24**, respectively. Substrates **25**–**28**[32,35] and **36**[32] were converted into the expected *endo*-trig products in good yields, except **29**, which was a product of an *exo*-trig cyclization. Obviously, the methoxy substituent influences the stabilization of the intermediate radical cation formed after the initial photooxidation by **14j** and which, of course, bears an unpaired spin and a charge. Normally, the unpaired spin is better stabilized at the benzylic position, which opens the way to an *endo*-trig cyclization. In this special case, the methoxy substituent stabilizes the cationic charge at the benzylic position leading to an *exo*-trig reaction. Product **41** was not obtained from substrate **39**.[16] Obviously, a phenolic hydroxy function cannot be used as a nucleophile in this photocatalytic method. This agrees with our previous studies with photocatalyst **14f**,[20] and is probably due to the difference in the acidities of phe-

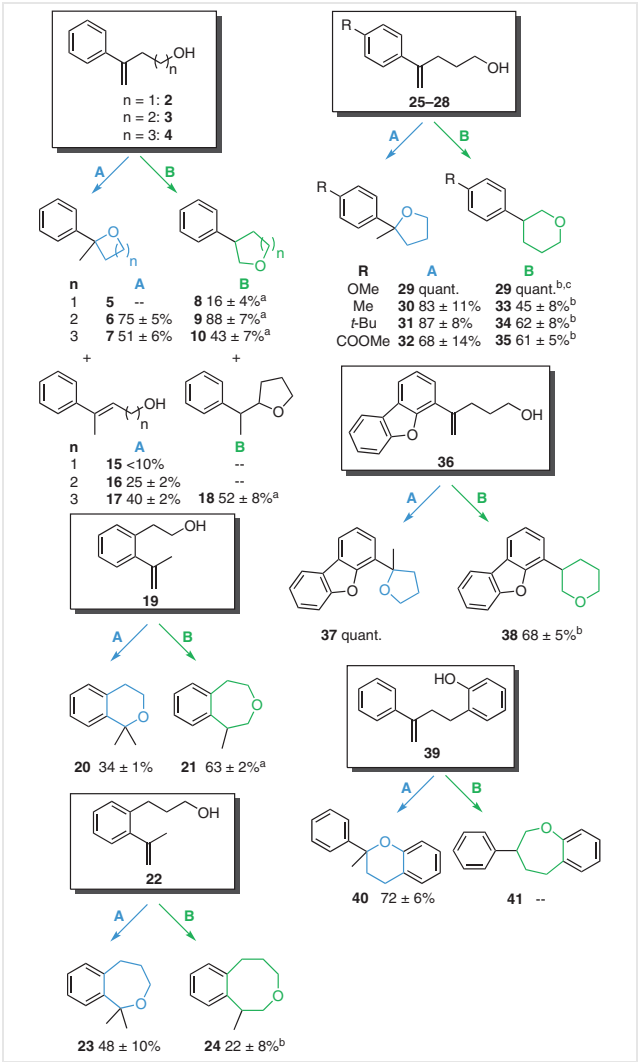

Figure 3 Substrates **2**–**4**, **19**, **22**, **25**–**28**, **36**, and **39** and their photocatalytic conversions into the *exo*-trig cyclized products **5**–**7**, **20**, **23**, **29**–**32**, **37**, and **40**; the *endo*-trig cyclized products **8**–**10**, **21**, **24**, **33**–**35**, **38**, and **41**; and the byproducts **15**–**17** and **18**. *Reaction conditions A*: substrate (164 mM), **1** (10 mol%), MeCN (0.75 mL), 35 °C, 365 nm LED, 65 h; *Reaction conditions B*: substrate (62 mM), **14j** (2 mol%), MeCN (2.00 mL), 35 °C, 525 nm LED. [a] 48 h. [b] 72 h.[31] [c] *exo*-trig product. The error ranges result from at least triplicate experiments, and are typical for photocatalytic conversions because the flat-bottomed glass vials used for the reactions are mass-produced products and have small manufacturing differences that give slightly different light intensities by reflection and transmission.

nols in comparison with alkyl alcohols, because the central cyclization step includes a proton transfer. Due to the long lifetime of the ground-state radical anions of biscyano-substituted perylene bisimides,[20] we were able to obtain evidence for the initial electron transfer in the proposed photocatalytic cycle by UV/vis absorption spectroscopy. When a reaction sample consisting of **14j** together with substrate **3** was irradiated for five minutes at 525 nm, the radical anion **14j**$^{-}$ was observed through its characteristic bands at 686 and 770 nm (SI; Figure S2). Thiophenol was omitted in this experiment to block the back electron transfer. Finally, we checked the photocatalytic activity of **14i** in comparison to the more soluble **14j** by irradiating substrate **26** with the maximum soluble concentration of **14i** (70 µM, 1.1 mol%). A conversion of 49% was achieved, whereas an experiment with **14j** (1.24 mM, 2 mol%) generated a conversion of 67%, supporting the idea that the more-soluble **PBI** is the more efficient photoredox catalyst.

In conclusion, the two presented variants are complementary parts of the photocatalytic toolbox with organic photoredox active chromophores. In the case of transition-metal complexes as photoredox catalysts, oxidative or reductive quenching is controlled by the choice of substrates and additional reagents. In our photocatalytic toolbox, the regioselectivity of the *endo*-trig versus *exo*-trig intramolecular cyclizations of bifunctional α-phenyl alkenes is controlled by the choice of the organic photoredox catalyst and the appropriate irradiation wavelength. The central photoredox catalytic reaction in both variants is an intramolecular nucleophilic addition of the hydroxy function to the olefin function. The *N*-arylphenothiazine **1** photocatalyzes the *exo*-trig cyclization to form five- and six-membered oxaheterocycles, whereas the perylene bisimide **14j** photocatalyzes the *endo*-trig cyclizations to give five-, six-, and seven-membered oxaheterocycles. The preliminary scope with 11 representative substrates presented here shows the complementarity and similarity of the two photocatalytic variants, together with the high potential of this photocatalytic toolbox as an important and more-sustainable alternative to transition-metal catalysis.

Conflict of Interest

The authors declare no conflict of interest.

Funding Information

Financial support by the Deutsche Forschungsgemeinschaft (grant Wa 1386/16-2) and KIT is gratefully acknowledged.

Acknowledgment

The authors thank the group of Professor Michael Meier (KIT) for sharing the GC infrastructure.

Supporting Information

Supporting information for this article is available online at https://doi.org/10.1055/s-0040-1719871.

References and Notes

(1) (a) Pagire, S. K.; Föll, T.; Reiser, O. *Acc. Chem. Res.* **2020**, *53*, 782. (b) Romero, N. A.; Nicewicz, D. A. *Chem. Rev.* **2016**, *116*, 10075. (c) McAtee, R. C.; McClain, E. J.; Stephenson, C. R. J. *Trends Chem.* **2019**, *1*, 111. (d) Marzo, L.; Paigre, S. K.; Reiser, O.; König, B. *Angew. Chem. Int. Ed.* **2018**, *57*, 10034. (e) Buzzetti, L.; Crisenza, G. E. M.; Melchiorre, P. *Angew. Chem. Int. Ed.* **2019**, *58*, 3730. (f) Capaldo, L.; Ravelli, D. *Eur. J. Org. Chem.* **2020**, 2783. (g) Ravelli, D.; Dondi, D.; Fagnoni, M.; Albini, A. *Chem. Soc. Rev.* **2009**, *38*, 1999.

(2) (a) Glaser, F.; Kerzig, C.; Wenger, O. S. *Angew. Chem. Int. Ed.* **2020**, *59*, 10266. (b) Rehm, T. H. *ChemPhotoChem* **2019**, *4*, 235; . (c) Strieth-Kalthoff, F.; James, M. J.; Teders, M.; Pitzer, L.; Glorius, F. *Chem. Soc. Rev.* **2018**, *47*, 7190. (d) Arias-Rotondo, D. M.; McCusker, J. K. *Chem. Soc. Rev.* **2016**, *45*, 5803.

(3) (a) Vega-Peñaloza, A.; Mateos, J.; Companyó, X.; Escudero-Casao, M.; Dell'Amico, L. *Angew. Chem. Int. Ed.* **2020**, *60*, 1082. (b) Bobo, M. V.; Kuchta, J. J.; Vannucci, A. K. *Org. Biomol. Chem.* **2021**, *19*, 4816. (c) Li, X.; Maffettone, P. M.; Che, Y.; Liu, T.; Chen, L.; Cooper, A. I. *Chem. Sci.* **2021**, *12*, 10742. (d) Zhang, Y.; Jiang, D.; Fang, Z.; Zhu, N.; Sun, N.; Liu, C.; Zhao, L.; Guo, K. *Chem. Sci.* **2021**, *12*, 9432. (e) Hutskalova, V.; Sparr, C. *Org. Lett.* **2021**, *23*, 5143.

(4) Hari, D. P.; König, B. *Chem. Commun.* **2014**, *50*, 6688.

(5) König, B.; Kümmel, S.; Cibulka, R. In *Chemical Photocatalysis*; König, B., Ed.; De Gruyter: Berlin, **2020**.

(6) Ghosh, I.; Marzo, L.; Das, A.; Shaikh, R.; König, B. *Acc. Chem. Res.* **2016**, *49*, 1566.

(7) Margrey, K. A.; Nicewicz, D. A. *Acc. Chem. Res.* **2016**, *49*, 1997.

(8) Zilate, B.; Fischer, C.; Sparr, C. *Chem. Commun.* **2020**, *56*, 1767.

(9) Mateos, J.; Rigodanza, F.; Vega-Peñaloza, A.; Sartorel, A.; Natali, M.; Bortolato, T.; Pelosi, G.; Companyó, X.; Bonchio, M.; Dell'Amico, L. *Angew. Chem. Int. Ed.* **2020**, *59*, 1303.

(10) Speckmeier, E.; Fischer, T. G.; Zeitler, K. *J. Am. Chem. Soc.* **2018**, *140*, 15353.

(11) Taeufer, T.; Hauptmann, R.; El-Hage, F.; Mayer, T. S.; Jiao, H.; Rabeah, J.; Pospech, J. *ACS Catal.* **2021**, *11*, 4862.

(12) Nikitas, N. F.; Gkizis, P. L.; Kokotos, C. G. *Org. Biomol. Chem.* **2021**, *19*, 5237.

(13) Taylor, R. D.; MacCoss, M.; Lawson, A. D. G. *J. Med. Chem.* **2014**, *57*, 5845.

(14) (a) Lee, K.-S.; Li, G.; Kim, S. H.; Lee, C.-S.; Woo, M.-H.; Lee, S.-H.; Jhang, Y.-D.; Son, J.-K. *J. Nat. Prod.* **2002**, *65*, 1707. (b) Alvarez, E.; Candenas, M.-L.; Perez, R.; Ravelo, J. L.; Delgado, M. *Chem. Rev.* **1995**, *95*, 1953.

(15) Ward, A. F.; Xu, Y.; Wolfe, J. P. *Chem. Commun.* **2012**, *48*, 609.

(16) Lu, Y.; Nakatsuji, H.; Okumura, Y.; Yao, L.; Ishihara, K. *J. Am. Chem. Soc.* **2018**, *140*, 6039.

(17) Alves, T. M. F.; Costa, M. O.; Bispo, B. A. D.; Pedrosa, F. L.; Ferreira, M. A. B. *Tetrahedron Lett.* **2016**, *57*, 3334.

(18) Kita, Y.; Yata, T.; Nishimoto, Y.; Yasuda, M. *J. Org. Chem.* **2018**, *83*, 740.

(19) Hu, N.; Li, K.; Wang, Z.; Tang, W. *Angew. Chem. Int. Ed.* **2016**, *55*, 5044.

(20) Weiser, M.; Hermann, S.; Wagenknecht, H.-A. *Beilstein J. Org. Chem.* **2015**, *11*, 568.

(21) (a) Hermann, S.; Wagenknecht, H.-A. *J. Pept. Sci.* **2017**, *23*, 563. (b) Hermann, S.; Sack, D.; Wagenknecht, H.-A. *Eur. J. Org. Chem.* **2018**, 2204.

(22) (a) Speck, F.; Rombach, D.; Wagenknecht, H.-A. *Beilstein J. Org. Chem.* **2019**, *15*, 52. (b) Rombach, D.; Wagenknecht, H.-A. *Angew. Chem. Int. Ed.* **2020**, *59*, 300. (c) Seyfert, F.; Mitha, M.; Wagenknecht, H.-A. *Eur. J. Org. Chem.* **2021**, 773.

(23) Ahrens, M. J.; Fuller, M. J.; Wasielewski, M. R. *Chem. Mater.* **2003**, *15*, 2684.

(24) **1,7-Dibromoperylene-3,4,9,10-tetracarboxylic Acid Bisimides 13a–j**; **General Procedure**
The appropriate amine RNH_2 (5.46 mmol, 3.00 equiv) was added to a solution of dibromide **12** (1.82 mmol, 1.00 equiv) in DMF (**13a–f**) or propionic acid (**13e–j**), and the mixture heated to 80 °C (**13a–f** in DMF) or under reflux (**13g–j** in propionic acid) for 15 h. In the case of **13i** and **13j**, ZnOAc (0.87 mmol, 0.04 equiv) was added. The solution was then cooled to r.t. and poured into H_2O. The resulting precipitate was collected by filtration and washed with H_2O. The crude product was purified by column chromatography (silica gel, CH_2Cl_2) to give a red solid; yield: 0.32–0.65 mmol (18–36%).

(25) **13j**
Red solid; yield: 0.32–0.65 mmol (31%) R_f = 0.7. ^{1}H NMR (500 MHz, $CDCl_3$): δ = 9.57 (d, *J* = 8.1 Hz, 2 H), 9.03 (s, 2 H), 8.81 (d, *J* = 8.1 Hz, 2 H), 7.52 (t, *J* = 7.8 Hz, 2 H), 7.37 (d, *J* = 7.8 Hz, 6 H), 2.84–2.54 (m, 4 H), 1.19 (d, *J* = 6.8 Hz, 24 H). ^{13}C NMR (126 MHz, $CDCl_3$): δ = 163.14, 162.64, 145.73, 138.62, 133.58, 133.41, 130.79, 130.25, 130.05, 129.77, 128.86, 127.83, 124.35, 123.32, 122.99, 121.20, 29.43, 24.18. HRMS (ESI): *m/z* [M$^+$] calcd for $C_{48}H_{40}Br_2N_2O_4$: 866.1355; found: 867.1431 [MH$^+$].

(26) Böhm, A.; Arms, H.; Henning, G.; Blaschka, P. DE 19547209, **1997**

(27) **1,7-Dicyanoperylene-3,4,9,10-tetracarboxylic Acid Bisimides 14a–j**; **General Procedure**
A suspension of the appropriate dibromo compound **13a–j** (0.76 mmol, 1.00 equiv), $Zn(CN)_2$ (7.55 mmol, 10.0 equiv), dppf (0.23 mmol, 0.30 equiv), and $Pd_2(dba)_3$ (0.23 mmol, 0.30 equiv) in anhyd 1,4-dioxane (40 mL) was refluxed under argon for 24 h. When the reaction was complete, the mixture was cooled to r.t. and filtered. The solvent was removed under reduced pressure, and the crude product was purified by column chromatography (silica gel, CH_2Cl_2) to afford a red solid; yield: 0.34–0.53 mmol (37–71%).

(28) **14j**
Red solid; yield: 0.34–0.53 mmol (65%); R_f = 0.2. ^{1}H NMR (500 MHz, $CDCl_3$): δ = 9.75 (d, *J* = 7.9 Hz, 2 H), 9.08 (s, 2 H), 9.03 (d, *J* = 8.1 Hz, 2 H), 7.54 (t, *J* = 8.3 Hz, 2 H), 7.38 (d, *J* = 7.8 Hz, 4 H), 2.82–2.58 (m, 4 H), 1.19 (d, *J* = 6.9, 2.0 Hz, 24 H). ^{13}C NMR (126 MHz, $CDCl_3$): δ = 162.77, 162.37, 161.93, 145.63, 138.56, 136.66, 134.17, 132.65, 132.08, 130.33, 129.71, 129.17, 127.39, 124.96, 124.48, 124.02, 119.11, 108.94, 29.52, 24.16. HRMS (ESI): *m/z* [M$^+$] calcd for $C_{50}H_{40}N_4O_4$: 760.3050; found: 760.3147 [MH$^+$].
Samples of **14a–i** contained small amounts of the corresponding 1,6-regioisomers, detectable by NMR spectroscopy, which could not be separated, but had almost the same optical and redox properties. See also: (a) Würthner, F.; Stepanenko, V.; Chen, Z.; Saha-Möller, C. R.; Kocher, N.; Stalke, D. *J. Org. Chem.* **2004**, *69*, 7933. (b) Dubey, R. K.; Efimov, A.; Lemmetyinen, H. *Chem. Mater.* **2011**, *23*, 778.

(29) **Determination of the Solubilities of 14a–j; General Procedure**
The extinction coefficients of **13a–j** were determined. The solubilities of the perylene bisimides were determined by preparing saturated solutions of them in pure MeCN at 25 °C. The solutions were filtered and their absorption was measured directly, or after further dilution when the optical density in the cuvette exceeded 1. The absorption spectroscopy was performed by using a Perkin Lambda 750 spectrometer with PTP 6 + 6 Peltier system and a Haake thermostat F4391 with 1 cm quartz-glass cuvettes (Starna) filled with a total volume of 1 mL.

(30) Ruoff, R. S.; Kadish, K. M.; Boulas, P.; Chen, E. C. M. *J. Phys. Chem.* **1995**, *99*, 8843.

(31) **Photochemical Reaction; General Procedure**
Irradiation of the photochemical reaction was carried out in a setup designed and manufactured by the University of Regensburg and the workshop of the Institute for Physical Chemistry at KIT; this was equipped with a Nichia NVSU233A LED and an Osram Oslon SSL 150 SMD LED. The reaction samples were irradiated from the bottom. The temperature of 35 °C was controlled by a thermostat (LAUDA Alpha R8). The appropriate hydroxy alkene and photoredox catalyst were suspended in MeCN, and the mixture was degassed four by four freeze–pump–thaw cycles then stirred at 35 °C for 48 or 65 h under an inert atmosphere with irradiation at 365 or 525 nm. The mixture was cooled to r.t. then purified and analyzed (see SI).

(32) Rösner, C.; Hennecke, U. *Org. Lett.* **2015**, *17*, 3226.

(33) (a) Baldwin, J. E. *J. Chem. Soc., Chem. Commun.* **1976**, 734. (b) Alabugin, I. V.; Gilmore, K.; Manoharan, M. *J. Am. Chem. Soc.* **2011**, *133*, 12608.

(34) **3-(2-Isopropenylphenyl)propan-1-ol (22); Typical Procedur**e
1-Bromo-2-isopropenylbenzene (3.49 g, 20 mmol, 1.0 equiv) was dissolved in dry THF (56 mL) under Ar, and the solution was cooled to –78 °C. A 1.6 M soln of BuLi in hexane (14 mL, 22 mmol, 1 equiv) was added dropwise over 15 min, and the mixture was stirred for 1.5 h at –78 °C. Oxetane (1.68 mL, 30 mmol, 1.5 equiv) was added dropwise to the mixture, and the mixture was stirred for 0.5 h at –78 °C, then warmed to r.t. The reaction was quenched with sat. aq NH_4Cl (25 mL) and the mixture was extracted with Et_2O. The collected organic layer was dried (Na_2SO_4) and concentrated, and the residue was purified by column chromatography [silica gel, hexane–EtOAc (4:1)] to give a colorless oil; yield: 1.53 g (17%).
^{1}H NMR (400 MHz, $CDCl_3$): δ = 7.24 – 7.04 (m, 4 H), 5.19 (s, 1 H), 4.85 (s, 1 H), 3.67 (q, J = 6.1 Hz, 2 H), 2.76 – 2.67 (m, 2 H), 2.05 (s, 3 H), 1.92 – 1.80 (m, 2 H), 1.30 (t, J = 5.5 Hz, 1 H).^{13}C NMR (101 MHz, $CDCl_3$): δ = 146.00, 143.87, 138.43, 129.23, 128.38, 127.14, 125.90, 115.03, 62.71, 34.69, 29.21, 25.39. HRMS (ESI): *m/z* [M$^+$] calcd for $C_{12}H_{16}O$ = 176.1201; found = 159.1166 [M – OH]$^+$.

(35) **Methyl 4-(1-Hydroxypent-4-en-1-yl)benzoate; Typical Procedure**
[4-(Methoxycarbonyl)phenyl]boronic acid (1.48 g, 12.0 mmol, 1.2 equiv), pent-4-yn-1-ol (0.93 mL, 10.0 mmol, 1.0 equiv.), $Pd(PPh_3)_4$ (347 mg, 0.30 mmol, 3 mol%), AcOH (0.11 mL, 2.00 mmol, 0.2 equiv), and anhyd 1,4-dioxane (30 mL) were stirred at 80 °C for 24 h. Purification by flash chromatography [silica gel, hexane–EtOAc (4:1)] gave a colorless solid; yield: 810 mg (4.99 mmol, 49%).
^{1}H NMR (400 MHz, $CDCl_3$): δ = 7.99 (d, *J* = 8.5 Hz, 2 H), 7.47 (d, *J* = 8.5 Hz, 2 H), 5.39 (s, 1 H), 5.19 (s, 1 H), 3.91 (s, 3 H), 3.67 (t, *J* = 6.2 Hz, 2 H), 2.62 (t, *J* = 7.9 Hz, 2 H), 1.86–1.64 (m, 2 H), 1.34 (br s, 1 H). ^{13}C NMR (101 MHz, $CDCl_3$) δ = 167.07, 147.34, 145.77, 129.83, 129.19, 126.22, 114.57, 62.42, 52.22, 31.49, 31.22. HRMS (ESI): *m/z* [M$^+$] calcd for $C_{13}H_{16}O_3$ = 220.1099; found = 221.1168 [MH$^+$].

(36) E_{red1}(**14j**/**14j**$^{\bullet-}$) = –0.15 V (vs. SCE); E_{00} = 2.3 eV.

(37) Hansch, C.; Leo, A.; Taft, R. W. *Chem. Rev.* **1991**, *91*, 165.